

NUCLEAR SPECIFIC HEAT AND PHASE TRANSITION IN FINITE NUCLEAR SYSTEMS

N. BOOMADEVI^a, J. DHIVYA SARANYA^a, S. SELVARAJ^b
T.R. RAJASEKARAN^a

^aDepartment of Physics, Manonmaniam Sundaranar University
Tirunelveli — 627012, Tamil Nadu, India

^bDepartment of Physics, The M.D.T. Hindu College
Tirunelveli — 627010, Tamil Nadu, India

*(Received April 2, 2013; revised version received August 8, 2013;
final version received February 28, 2014)*

A statistical theory incorporating temperature, angular momentum and deformation degrees of freedom for complex nuclear system has been developed. An investigation for nuclear specific heat as a function of temperature and angular momentum is provided. The occurrence of a peak structure in the specific heat at temperatures of the order of 2.0–3.0 MeV confirms the phase transitions for seven even–even $2s$ – $1d$ shell nuclei.

DOI:10.5506/APhysPolB.45.989

PACS numbers: 05.70.Fh, 65.40.Ba, 21.10.Ma, 27.30.+t

1. Introduction

In recent years, phase transition in a nucleus has been an important phenomenon in the study of nuclear properties [1, 2]. Nuclei are a finite quantum system, which has unique transitional features. In nuclei, two types of phase transitions occur: *(i)* pairing phase transition (superfluid to normal fluid) and *(ii)* shape-phase transition (deformed to spherical shape). The second type of phase transitions is also called quantum phase transitions. Quantum phase transitions have also been extended to excited state, which is a qualitative change in the properties of the system as a function of the excitation energy [3]. The phase transitions in finite nuclei have been measured by many physicists from the experimental [4] and theoretical [5–7] point of view.

The vanishing of an order parameter such as the gap parameter in superfluid nuclei and the quadrupole moment in the deformed nuclei has been offered as evidence for the existence of a phase transition in such systems [8, 9].

The phase transition from superfluid to normal nuclear matter has been elaborately investigated in the determination of single particle level density parameter as a function of angular momentum and temperature reported in Ref. [10]. In the present study, we have extended our investigation of nuclear phase transitions in light nuclei, with particular focus to its geometrical forms. The nuclear specific heat is also one among them to study the existence of phase transition.

One important tool to study the phase transition is the specific heat. The specific heat is recognized as a quantity which indicates the occurrence of phase transition. The nuclear specific heat of a fused compound system formed in heavy ion collision can be estimated if the excited states spectrum is well-known. Elementary examples of this are stated by Pathria [11], including the free particle, the harmonic oscillator and rigid rotor. The behavior of nuclear specific heat at high temperature directly yields the information about the relevant degrees of freedom in the spectrum of Dulong and Petit's law. Tanabe, Goodman, Cole, Miller and others [12–21] have emphasized the role of nuclear specific heat in the determination of important properties of the nuclei. One motivating feature is the peak structure in specific heat which endorses the existence of phase transition [22]. It is the aim of this paper to study the interplay between specific heat and phase transition in finite nuclear systems.

Several authors have extensively investigated [12, 15–21] the subsistence of phase transition in finite nuclei. Miller *et al.* [16] have envisaged the occurrence of phase transition using finite temperature Hartree–Fock (FTHF) approximation and in the exact canonical ensemble. Rossignoli *et al.* [23] have investigated the correlation between thermal effects and two of the crucial ingredients of the many body problem, via superconductivity and deformation due to a long-range residual force. They have also presented a finite temperature projection method which exhibits important shortcomings such as the prediction of sharp phase transition [24].

Until the present, a foremost activity has been accomplished using the interacting boson model (IBM) for the study of phase transitions [25]. On the other hand, various cranking Hartree–Fock–Bogoliubov (CHFb) calculations provide a reliable analysis for medium and heavy systems [26]. In recent times, a self consistent mean field calculations combined with the random phase approximation (RPA) analysis are beneficial to detect quantum phase transitions [27]. In contrary, analogous investigations have shown that the proposed phase transition does not occur for some nuclei belonging to the $2s-1d$ shell [19].

The appearance of peaks in the specific heat at temperatures $T = 1.7$ MeV and 3.1 MeV for the nuclei ^{24}Mg corresponding to average change in shape of the nucleus from ellipsoidal to axially symmetric and from axially symmetric

to spherically symmetric shapes, emerge as a signal for phase transitions [17]. Hasegawa *et al.* [28] have witnessed shape phase transition in $A \approx 70$ nuclei along the $N \approx Z$ line. This occurrence of phase transition to deformed nuclei is due to the strong proton–neutron correlations in these nuclei. Civitarese *et al.* [20] have reported that the occurrence of a bump in the specific heat in some of the light nuclei belonging to the $2s-1d$ shell using nuclear SU_3 model, may be due to finite size effect rather to a phase transition. Thermal excitation induces change in the nuclear shape related to this phase transition and the peak in specific heat appears due to change in level density allied with thermal excitation.

It is really interesting and open question whether or not phase transitions do occur in finite nuclear system at finite temperatures and signatures of these phase transitions remain despite of fluctuations [29]. The finite temperature mean field theories such as Bardeen–Cooper–Schrieffer (BCS) [30], Hartree–Fock (HF) [31], and Hartree–Fock–Bogoliubov (HFB) [32, 33] have been addressed the phase transition from superfluid to normal fluid nuclear matter. Esashika *et al.* [34] have studied the influence of number and number parity projections on heat capacities of nuclear systems ^{161}Dy and ^{162}Dy using finite temperature BCS theory and found S-shaped heat capacity at temperature T less than the critical temperature T_c , that corresponds to the superfluid to normal phase transition. Using the shell model Monte Carlo approach, the signatures of both pairing and shape–phase transition in the families of even–even rare earth samarium and neodymium isotopes were found in collective enhancement factors of level densities by Ozen *et al.* [35]. Even so, empirical analysis of experimental observation does not prognosticate an abrupt phase transition, the cause being disregard of fluctuation in the mean field approximations. The quantal and statistical fluctuations are necessary in identifying phase transitions in light nuclear systems. Within the framework of static path approximation (SPA) plus random phase approximation (RPA) treatment, Rossignoli *et al.* [36] have investigated thermal and quantal fluctuations and even–odd effects in nuclear systems ^{164}Er and ^{165}Er at finite temperature. Evaluating RPA correction to SPA they have found the smoothing of the BCS transition and the even–odd effects in the pairing energy and specific heat. Liu and Alhassid [37] have developed a new method for calculating the heat capacity using the shell model Monte Carlo (SMMC) approach, for iron isotopes $^{52-62}\text{Fe}$, and identified a signature of phase transition in the heat capacities despite the large fluctuations. Strictly speaking, quantal and statistical fluctuations are of essential importance since they smooth out the singularities allied with phase transitions [38]. In the statistical theory, the equilibrium shape of the nucleus at given angular momentum and temperature has been obtained by minimizing the free energy as a function of deformation. Therefore, our statistical

approach to establish the existence of phase transition in finite light nuclei is consistent with mean field theories which render the thermodynamical limit. Consequently, our statistical approach does not take into account the effect of shape fluctuations. However, the statistical theory incorporates the deformation degrees of freedom, collective and non-collective rotation is used to verify further that a phase transition has indeed occurred for nuclei with $20 \leq A \leq 30$. This theory has been used in the evaluation of single particle level density parameter [39], neutron separation energy and emission probability at high spins [40].

Moretto [41] promoted the statistical model by using the single-particle levels of deformed nuclei. Statistical calculations are performed using the grand-canonical ensemble. The determinations of grand partition function of the system are based on the conservation of energy, number of particles and angular momentum projection along the z -axis. In the present manuscript, calculations have been performed on the nuclear specific heat for the light nuclei such as: ${}^{20}_{10}\text{Ne}$, ${}^{22}_{10}\text{Ne}$, ${}^{24}_{10}\text{Ne}$, ${}^{24}_{12}\text{Mg}$, ${}^{26}_{12}\text{Mg}$, ${}^{28}_{14}\text{Si}$, and ${}^{30}_{14}\text{Si}$. It shows the presence of a bump at T of the order of 2.0 to 3.5 MeV for all the light nuclei. The results obtained from our calculations are similar to reported in [17, 20, 38].

The atomic nucleus comprises a unique system in that it exhibits both microscopic features [42] and statistical aspects generally explained in terms of level density [43]. The nuclear level density as a function of excitation energy is an important fundamental property which is used to derive all thermodynamical quantities such as entropy and specific heat of the excited nuclei. Moreover, it provides a strongest test for nuclear models [44]. Since the phase-space governs the properties of a large class of nuclear reactions, a precise knowledge of level density is essential for understanding the nuclear reactions. At higher excitation energies, the nuclear level density increases so rapidly that it is practically impossible to study the transition between the levels and hence a statistical description becomes adequate. Level density formalisms have been developed and applied both to schematic and realistic single-particle spectra. Most calculations of nuclear level densities are extensions and modifications of the Fermi gas model to which pairing and shell effects are added semi-empirically [45]. Such an approach has led to a quantitative understanding of the disappearance of the shell effects with increasing excitation energy. This feature, contained in the statistical theory, has been used to calculate the ground-state shell effects as an alternative to the Strutinsky method [46].

For higher excitation energy, one can use models such as the back-shifted Fermi gas (BSFG) model [4], the constant temperature (CT) model [47] or the interacting shell model (ISM) [48]. The ISM is a good microscopic model for the calculations of level densities since it includes both shell

effects and residual interactions. The statistical properties of nuclei using the shell model Monte Carlo method are calculated by Mocelj *et al.* [49]. Many approaches make use of a phenomenological treatment such as the macroscopic–microscopic finite range droplet model [50]. But a consistent microscopic description of all the required properties of nuclei is still not feasible. Thus in this paper, we tried to have a better understanding of phase transition using the statistical theory of hot rotating nuclei (STHR). The behavior of the excitation energy, specific heat and nuclear level density, and level density parameter are extracted. However, our main focus is on specific heat and phase transition, the results of level density parameter are not presented. It is found that the calculated values of level density parameter very well reproduce the empirical relation $A/8$ or $A/10$.

In Sec. 2 the formalism is used to describe the nuclear specific heat and level density. The results and discussions are given in Sec. 3.

2. Formalism

Statistical descriptions of finite nuclear systems are generally based on grand canonical ensemble averages. For various events, one often needs a statistics with good quantum numbers like angular momentum or particle number, which requires a use of constrained ensembles. The common procedure consists in determining first the grand partition function of the system and then in restricting it in such a way, so as to conserve energy, number of particles and angular momentum. The basic ingredient to the statistical theory is a suitable shell model level scheme. The method of obtaining the single particle energy levels using the deformed Nilsson Hamiltonian is briefly given below.

The Hamiltonian for the deformed Nilsson oscillator [51] is given by

$$H = \frac{p^2}{2m} + \left(\frac{m}{2}\right) (\omega_x^2 x^2 + \omega_y^2 y^2 + \omega_z^2 z^2) + C\bar{l}.\bar{s} + D \left(\bar{l}^2 - 2\langle\bar{l}^2\rangle\right), \quad (1)$$

with $C = 2\kappa\hbar\omega_0$ and $D = \kappa\mu\hbar\omega_0$. Here, ω_0 is the harmonic oscillator parameter that involves the principle of volume conservation for nuclei deformed from spherical shapes. ω_x , ω_y , and ω_z are the three oscillator frequencies with the constraint that the total volume remains constant such that

$$\omega_x\omega_y\omega_z = \omega_0^3 = \text{constant}. \quad (2)$$

The coefficients for the $\bar{l}.\bar{s}$ and $\bar{l}^2 - 2\langle\bar{l}^2\rangle$ terms are taken from Seeger [52] who has fitted them to produce the shell corrections to ground-state masses.

The value of undeformed oscillator spacing $\hbar\omega_0 = 41 \text{ MeV}/(A^{1/3} + 0.77)$ is used in our level scheme and the κ and μ values are taken from Ref. [53]. The single particle energies ϵ_i and spin projections m_i as a function of deformation parameter δ are obtained by diagonalizing the Nilsson Hamiltonian in cylindrical basis. The single particle energies are generated up to $N = 11$ levels which are found to be sufficient for the range of temperatures used in the present study. The required angular momenta are generated by introducing the z projection of the angular momentum as a constant of motion through the Lagrangian multiplier γ corresponding to the single-particle spins m_i [40, 41]. Calculations are carried out by varying deformation parameter δ values in steps of 0.1 from -0.6 (oblate) to 0.6 (prolate).

2.1. Statistical theory

The statistical properties of the system are contained in the grand partition function which is given by [41]

$$\begin{aligned} \ln Q = & \sum_i \ln [1 + \exp (\alpha_N + \gamma m_i^N - \beta \epsilon_i^N)] \\ & + \sum_i \ln [1 + \exp (\alpha_Z + \gamma m_i^Z - \beta \epsilon_i^Z)] , \end{aligned} \quad (3)$$

where the Lagrange multipliers α_N , α_Z , β , and γ conserve the number of neutrons, protons, total energy for a temperature $T = 1/\beta$ and the angular momentum of the system respectively and are fixed by the following equations

$$\langle N \rangle = \frac{\partial \ln Q}{\partial \alpha_N} , \quad (4)$$

$$\langle Z \rangle = \frac{\partial \ln Q}{\partial \alpha_Z} , \quad (5)$$

$$\langle I \rangle = \frac{\partial \ln Q}{\partial \gamma} , \quad (6)$$

$$\langle E \rangle = -\frac{\partial \ln Q}{\partial \beta} . \quad (7)$$

The single particle levels for the neutrons ϵ_i^N with spin projection m_i^N and protons ϵ_i^Z with the spin projection m_i^Z are obtained from the Nilsson Hamiltonian. The particle number equations for neutrons, protons and the corresponding equations for angular momentum I and energy E are given below [40]

$$N = \sum_i n_i^N , \quad (8)$$

$$Z = \sum_i n_i^Z, \quad (9)$$

$$I = \sum_i m_i^N n_i^N + \sum_i m_i^Z n_i^Z, \quad (10)$$

$$E(I, T) = \sum_i \epsilon_i^N n_i^N + \sum_i \epsilon_i^Z n_i^Z. \quad (11)$$

The entropy is calculated using the relation

$$\begin{aligned} S(I, T) = & -\sum_i [n_i^N \ln n_i^N + (1 - n_i^N) \ln (1 - n_i^N)] \\ & -\sum_i [n_i^Z \ln n_i^Z + (1 - n_i^Z) \ln (1 - n_i^Z)]. \end{aligned} \quad (12)$$

Equations (8), (9) and (10) have to be solved to determine α_N , α_Z and γ for each temperature $T = 1/\beta$. The excitation energy $E^*(I, T)$ is obtained using the relation

$$E^*(I, T) = E(I, T) - E_0, \quad (13)$$

where E_0 is the ground state energy of the system. The specific heat C_V as a function of angular momentum I and temperature T is given as

$$C_V(I, T) = T \frac{dS(I, T)}{dT}, \quad (14)$$

or

$$C_V(I, T) = \frac{dE(I, T)}{dT}. \quad (15)$$

The nuclear level density [54] for various excitation energies and angular momentum is given by

$$\rho(E^*) = \frac{(\hbar^2/2\theta)^{\frac{3}{2}} (2I + 1) \sqrt{a} \exp\left(2\sqrt{aE^*}\right)}{12(E^* + T)^2}, \quad (16)$$

where a is the single particle level density parameter and θ is the rigid body moment of inertia. This expression has been already used in our calculation of single neutron emission probability for fused compound system of ^{156}Er [39] and the results obtained agree very well with the experimental data of Henss *et al.* [55]. The free energy of the hot rotating system contains all the thermodynamic information and is computed as

$$F(I, T) = E(I, T) - TS. \quad (17)$$

The minimisation of the above expression with respect to the deformation parameter δ determines the equilibrium shape of the nucleus as a function of angular momentum and temperature [6]. The parameters like total energy, excitation energy, specific heat, level density and level density parameter are computed as a function of angular momentum I , temperature T . The range of the angular momentum and temperature are considered in our calculations as $I = 0$ to $16 \hbar$ and $T = 0.5$ MeV to 6 MeV respectively. All the curves are drawn in Figs. 1–11, after minimizing the free energy with respect to the deformation parameter.

3. Results and discussion

In this work, we have offered certain evidences for the occurrence of phase transition in light nuclei belonging to the $2s-1d$ shell. The numerical results of excitation energy E^* as a function of temperature T and angular momentum I for the nuclei $^{20}_{10}\text{Ne}$, $^{22}_{10}\text{Ne}$, $^{24}_{12}\text{Mg}$, and $^{28}_{14}\text{Si}$ are shown in Figs. 1 and 2 with a change in slope at certain regions for all the nuclei. Figure 1 shows a rapid change of slope for $I = 0\hbar$ at $T \approx 3.5$ MeV for all the four nuclei. This consents moderately with a critical temperature of about 3.1 MeV for the ensemble average of energy obtained in FTHF calculations of Miller *et al.* [16]. They have found a change in slope at $T \approx 1.7$ MeV and $T \approx 3.1$ MeV for $^{24}_{12}\text{Mg}$. Similar effects are seen for $^{24}_{12}\text{Mg}$, at $I = 0\hbar$ with the change in the slope at $T \approx 3.7$ MeV and for $^{28}_{14}\text{Si}$ shows transformations at $T \approx 1.5$ MeV

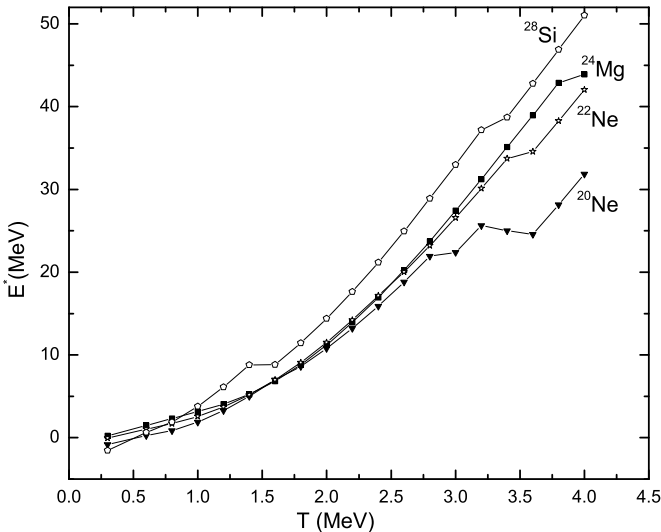


Fig. 1. The excitation energy E^* as a function of temperatures T at the angular momentum $I = 0\hbar$ for ^{20}Ne , ^{22}Ne , ^{24}Mg and ^{28}Si .

and $T \approx 3.0$ MeV. Usually, a change in the slope at $T \approx 1.5$ MeV implies a change in the system from a triaxial to an axially symmetric shape and a change at $T \approx 3.0$ MeV signifies a deformed to spherical phase transition [16, 38]. Therefore, for all the four nuclei considered, one can see a sudden transformation at $T \approx 3.5$ MeV (Fig. 1) which can be interpreted as evidences for phase transition.

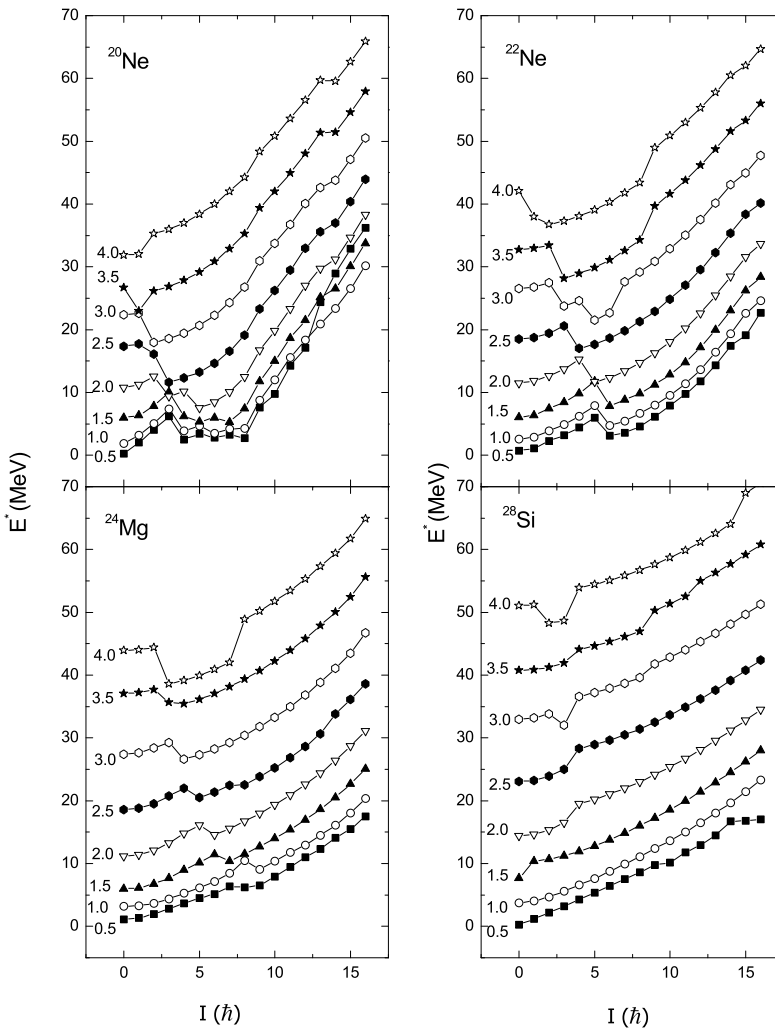


Fig. 2. The excitation energy E^* as a function of angular momentum I for various temperatures T for ^{20}Ne , ^{22}Ne , ^{24}Mg and ^{28}Si . The numbers on the curve refer to the temperature in units of MeV.

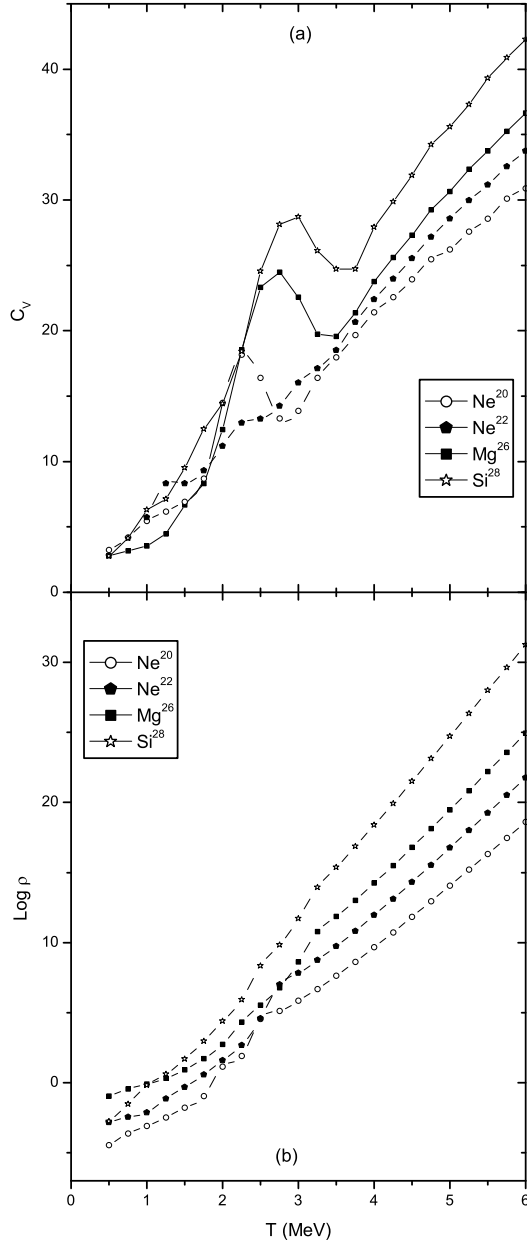


Fig. 3. (a) The nuclear specific heat C_V as a function of temperature T at the angular momentum $I = 0\hbar$ for ^{20}Ne , ^{22}Ne , ^{24}Mg , and ^{28}Si . (b) The nuclear level density ρ as a function of temperature at the angular momentum $I = 0\hbar$ for ^{20}Ne , ^{22}Ne , ^{24}Mg , and ^{28}Si .

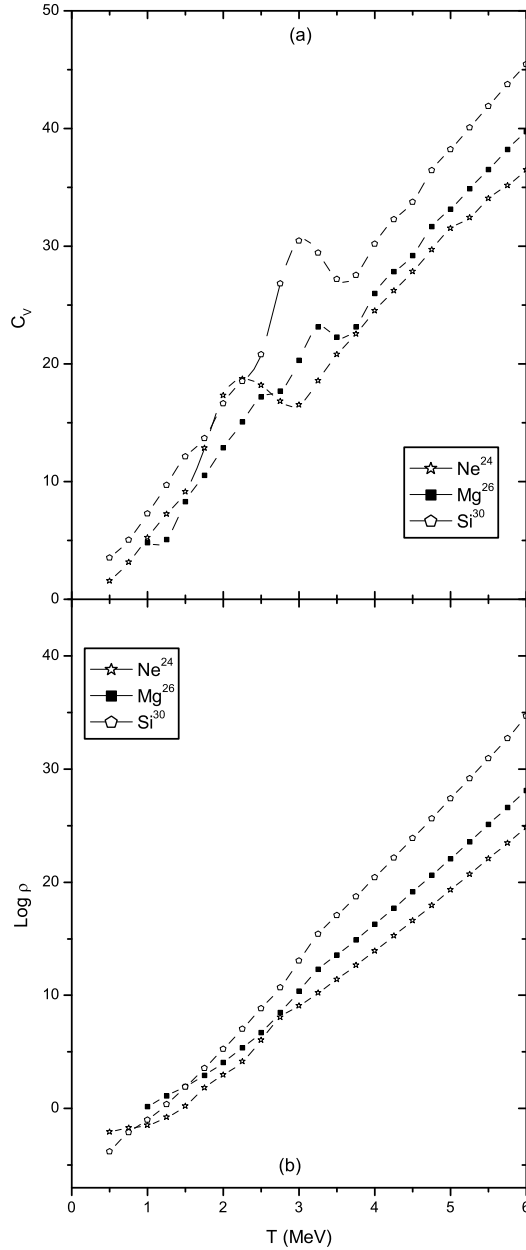


Fig. 4. (a) The nuclear specific heat C_V as a function of temperature T at the angular momentum $I = 0\hbar$ for ^{24}Ne , ^{26}Mg , and ^{30}Si . (b) The nuclear level density ρ as a function of temperature at the angular momentum $I = 0\hbar$ for ^{24}Ne , ^{26}Mg , and ^{30}Si .

Specific heat and level density calculations are executed for all the seven even-even $2s$ - $1d$ shell nuclei considered in the text. The nuclear specific heat C_V dependent on the temperature for $I = 0\hbar$ is presented in Fig. 3 (a) for ${}^{20}_{10}\text{Ne}$, ${}^{22}_{10}\text{Ne}$, ${}^{24}_{12}\text{Mg}$, and ${}^{28}_{14}\text{Si}$ and in Fig. 4 (a) for ${}^{24}_{10}\text{Ne}$, ${}^{26}_{12}\text{Mg}$, and ${}^{30}_{14}\text{Si}$. All the nuclei have a general tendency to exhibit an abrupt change in the specific heat beyond temperature 1.5 MeV. The peak in specific heat occurs at different temperatures for different nuclei.

In Fig. 3 (a) the peak appears at $T \approx 2.25$ MeV for ${}^{20}_{10}\text{Ne}$ and ${}^{22}_{10}\text{Ne}$, at $T \approx 2.75$ MeV for ${}^{24}_{12}\text{Mg}$ and at $T \approx 3.0$ MeV for ${}^{28}_{14}\text{Si}$. Figure 4 (a) shows the peak at $T \approx 2.25$ MeV for ${}^{24}_{10}\text{Ne}$, $T \approx 3.25$ MeV for ${}^{26}_{12}\text{Mg}$ and $T \approx 3.0$ MeV for ${}^{30}_{14}\text{Si}$. The bump in specific heat at T between 2.0 and 4.0 MeV is analogous to the one reported in [20] for all the light nuclei. Miller *et al.* [17] have computed specific heat for ${}^{20}_{10}\text{Ne}$ using the canonical ensemble from the eigenstates of different effective interactions. They have pointed out analogous peak in specific heat at $T \approx 2.1$ MeV in FTHF approximation for the Vary–Yang interaction signifying that a deformed-to-spherical phase transition has taken place. Thus we note that with increasing temperature, the appearance of prominent peak in specific heat for all the nuclei can be interpreted as the signature of phase transition associated with a change in nuclear shape.

However, the peak, as shown in a canonical ensemble calculations of the specific heat in ${}^{24}_{12}\text{Mg}$ [16, 17, 20], which occurs at low temperature ($T \approx 0.5$ MeV) does not appear in the present work. If specific heat is calculated using the states in the ground state rotational band alone, the

TABLE I

The $C_V(I, T)$ as a function of angular momentum and temperature for ${}^{20}\text{Ne}$.

T [MeV]	Specific heat C_V				
	$I = 0\hbar$	$I = 4\hbar$	$I = 8\hbar$	$I = 12\hbar$	$I = 16\hbar$
.50	3.26	1.42	1.40	1.09	4.59
1.00	5.44	6.13	3.26	3.78	6.53
1.50	6.94	3.95	7.34	7.08	8.77
2.00	14.48	9.25	11.18	10.18	11.29
2.50	16.40	13.87	14.28	13.26	14.19
3.00	13.87	16.91	17.34	15.78	16.71
3.50	17.95	19.62	19.72	18.98	19.13
4.00	21.42	22.80	22.80	21.26	21.65
4.50	23.95	24.51	24.63	23.83	24.17
5.00	26.23	26.23	26.55	25.91	26.40
5.50	28.56	28.56	29.75	28.18	28.61
6.00	30.88	30.88	30.42	30.23	30.46

smaller peak at the lower temperature can be effectively reproduced [16]. It has to be taken into account that the larger peak in specific heat will not be noticed, if only the states in the ground state rotational band alone are considered. Tables I–VII give the specific heat as a function of temperature and angular momentum for all the seven nuclei.

TABLE II

The $C_V(I, T)$ as a function of angular momentum and temperature for ^{22}Ne .

T [MeV]	Specific heat C_V				
	$I = 0\hbar$	$I = 4\hbar$	$I = 8\hbar$	$I = 12\hbar$	$I = 16\hbar$
.50	.69	1.70	2.08	.81	3.10
1.00	5.73	4.81	4.45	4.34	6.34
1.50	8.31	6.80	6.67	9.08	9.36
2.00	11.17	10.38	10.75	11.81	13.10
2.50	12.97	13.49	14.72	15.44	16.34
3.00	16.03	15.82	18.07	17.86	19.15
3.50	18.51	19.80	21.29	20.70	21.58
4.00	22.38	22.88	23.61	23.68	24.38
4.50	25.54	25.96	26.38	25.88	26.81
5.00	28.56	28.70	29.12	28.74	29.59
5.50	31.17	31.17	32.16	31.15	31.46
6.00	33.76	33.76	34.32	33.56	33.67

TABLE III

The $C_V(I, T)$ as a function of angular momentum and temperature for ^{24}Ne .

T [MeV]	Specific heat C_V				
	$I = 0\hbar$	$I = 4\hbar$	$I = 8\hbar$	$I = 12\hbar$	$I = 16\hbar$
.50	1.56	2.41	1.56	2.75	1.92
1.00	5.22	7.55	4.32	6.69	5.97
1.50	9.11	8.60	10.02	10.25	10.51
2.00	17.30	11.11	11.78	13.93	14.19
2.50	18.18	17.43	15.52	17.38	17.25
3.00	16.52	18.26	19.29	20.44	20.94
3.50	20.79	19.21	22.41	23.50	23.63
4.00	24.51	22.89	25.57	26.46	26.95
4.50	27.85	26.20	28.48	29.39	29.39
5.00	31.51	29.68	30.98	32.22	32.22
5.50	34.07	32.42	34.07	34.68	34.55
6.00	36.49	35.17	36.49	36.76	36.76

TABLE IV

The $C_V(I, T)$ as a function of angular momentum and temperature for ^{24}Mg .

T [MeV]	Specific heat C_V				
	$I = 0\hbar$	$I = 4\hbar$	$I = 8\hbar$	$I = 12\hbar$	$I = 16\hbar$
.50	2.79	1.19	4.03	2.85	4.62
1.00	3.55	4.14	5.77	5.76	8.04
1.50	6.68	8.76	7.72	9.78	11.86
2.00	12.46	10.54	12.90	14.28	14.55
2.50	23.32	13.37	14.56	17.78	18.11
3.00	22.56	21.37	18.86	20.75	20.94
3.50	19.58	19.14	22.28	23.60	23.89
4.00	23.76	24.19	25.67	26.58	27.08
4.50	27.31	28.09	28.45	29.79	29.65
5.00	30.63	31.07	31.30	32.25	32.22
5.50	33.76	33.79	34.15	34.43	34.81
6.00	36.66	36.66	36.66	37.03	37.25

TABLE V

The $C_V(I, T)$ as a function of angular momentum and temperature for ^{26}Mg .

T [MeV]	Specific heat C_V				
	$I = 0\hbar$	$I = 4\hbar$	$I = 8\hbar$	$I = 12\hbar$	$I = 16\hbar$
.50	3.82	2.78	2.13	4.16	3.63
1.00	4.81	5.94	5.20	7.06	7.63
1.50	8.29	9.28	12.13	11.87	11.87
2.00	12.87	15.46	12.87	14.57	15.44
2.50	17.18	15.82	16.81	17.99	18.98
3.00	20.29	21.16	19.93	23.67	22.68
3.50	22.25	23.14	23.88	25.53	25.65
4.00	25.99	26.49	27.35	29.23	28.93
4.50	29.21	29.45	30.57	32.05	31.63
5.00	33.16	33.16	33.79	34.90	34.60
5.50	36.51	36.51	36.87	37.61	37.61
6.00	39.72	39.72	39.72	40.43	40.43

TABLE VI

The $C_V(I, T)$ as a function of angular momentum and temperature for ^{28}Si .

T [MeV]	Specific heat C_V				
	$I = 0\hbar$	$I = 4\hbar$	$I = 8\hbar$	$I = 12\hbar$	$I = 16\hbar$
.50	2.77	1.13	2.34	4.06	3.78
1.00	6.32	6.53	6.74	8.17	7.63
1.50	9.50	12.47	11.30	12.17	12.17
2.00	14.44	22.18	16.61	16.28	16.58
2.50	24.56	22.34	20.38	19.98	20.28
3.00	28.70	20.96	22.76	23.97	24.09
3.50	24.73	24.14	25.73	27.36	27.67
4.00	27.91	28.28	28.12	30.91	31.21
4.50	31.88	31.67	33.05	34.60	34.60
5.00	35.61	35.44	36.61	37.46	37.46
5.50	39.30	39.34	40.03	40.73	40.43
6.00	42.27	42.46	43.27	43.01	43.29

TABLE VII

The $C_V(I, T)$ as a function of angular momentum and temperature for ^{30}Si .

T [MeV]	Specific heat C_V				
	$I = 0\hbar$	$I = 4\hbar$	$I = 8\hbar$	$I = 12\hbar$	$I = 16\hbar$
.50	3.51	2.72	3.18	5.05	2.72
1.00	7.29	7.43	7.62	8.62	7.83
1.50	12.12	12.81	12.45	13.11	12.94
2.00	16.62	20.94	18.89	17.76	17.60
2.50	20.79	23.21	19.92	22.12	21.96
3.00	30.46	23.91	24.24	25.99	25.82
3.50	27.20	26.51	27.53	29.23	29.07
4.00	30.19	30.19	31.88	33.42	32.97
4.50	33.77	33.77	35.04	36.83	36.83
5.00	38.22	38.22	40.59	41.65	40.57
5.50	41.88	41.88	42.36	43.48	43.48
6.00	45.44	45.44	45.54	46.43	46.43

Figures 3 (b) and 4 (b) illustrate the results of level density calculations with a slight change around the critical temperature for all the seven nuclei. One can clearly see that the slender change in the level density coincides with the peaks in the specific heat at the higher temperature. Thus, the peaks in the specific heat in all cases are the result of the changes in the many body level density around the critical temperature [56].

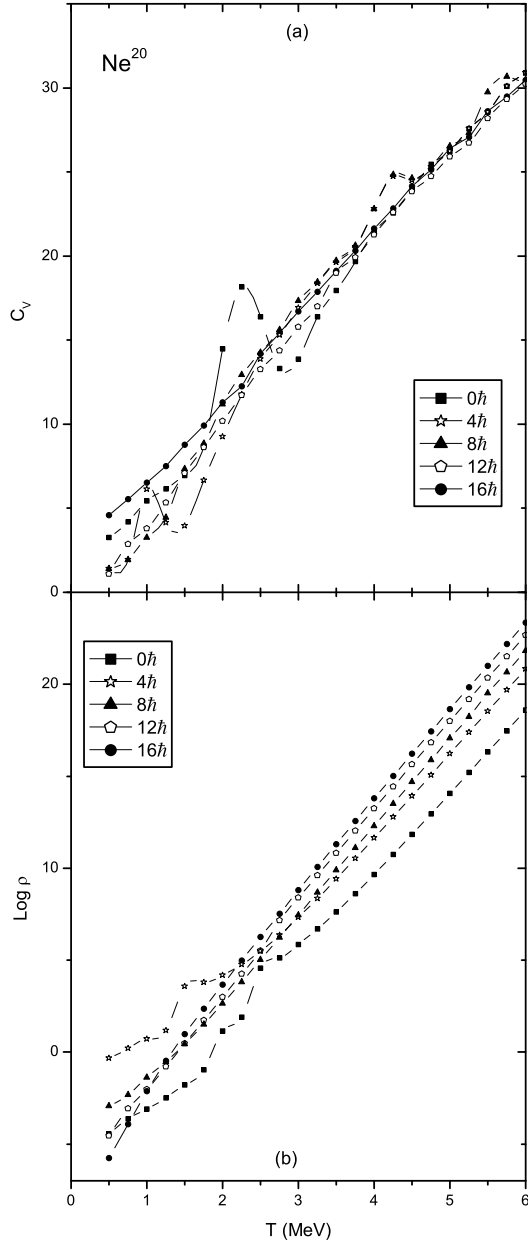


Fig. 5. (a) The nuclear specific heat C_V as a function of temperature T and angular momentum I for ^{20}Ne . (b) The nuclear level density ρ as a function of temperature and angular momentum for ^{20}Ne .

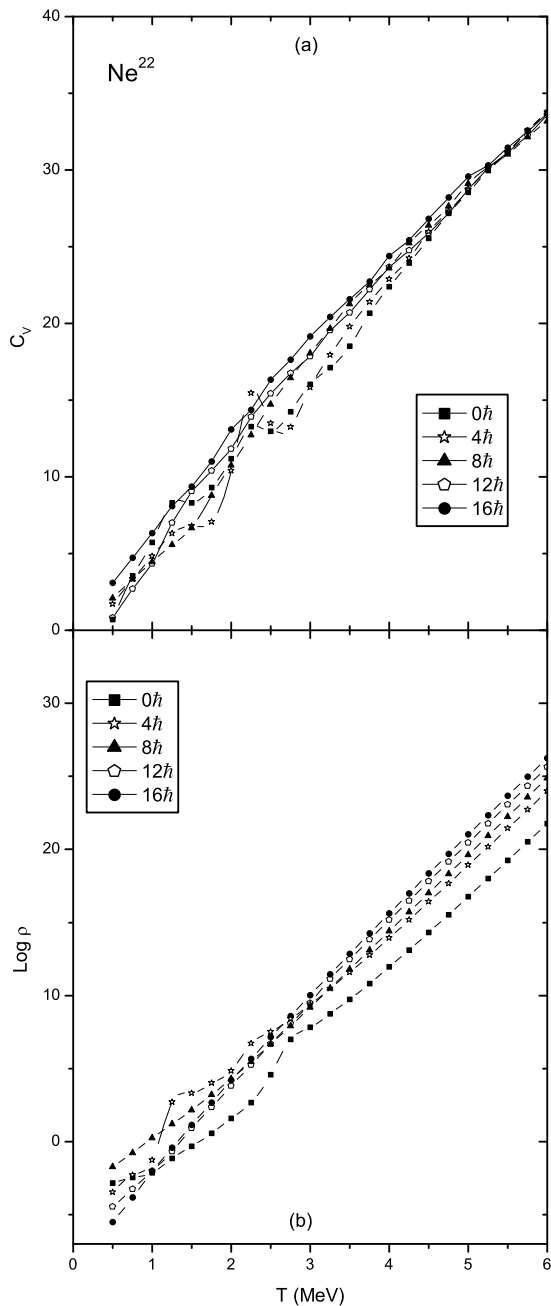


Fig. 6. (a) As in Fig. 5 (a) for ^{22}Ne . (b) As in Fig. 5 (b) for ^{22}Ne .

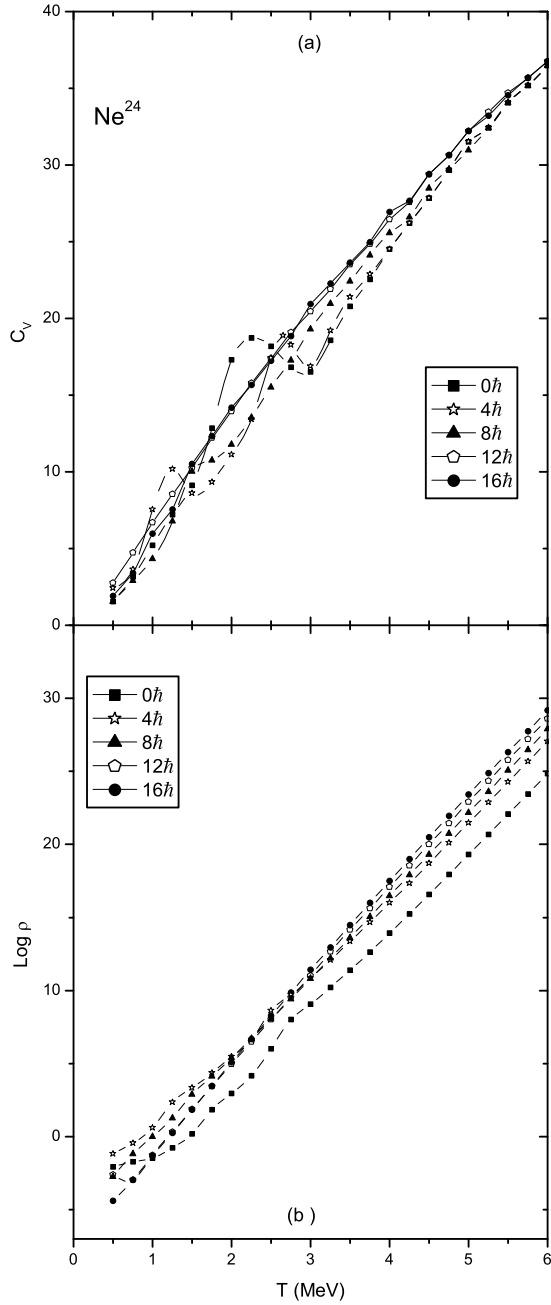


Fig. 7. (a) As in Fig. 5 (a) for ^{24}Ne . (b) As in Fig. 5 (b) for ^{24}Ne .

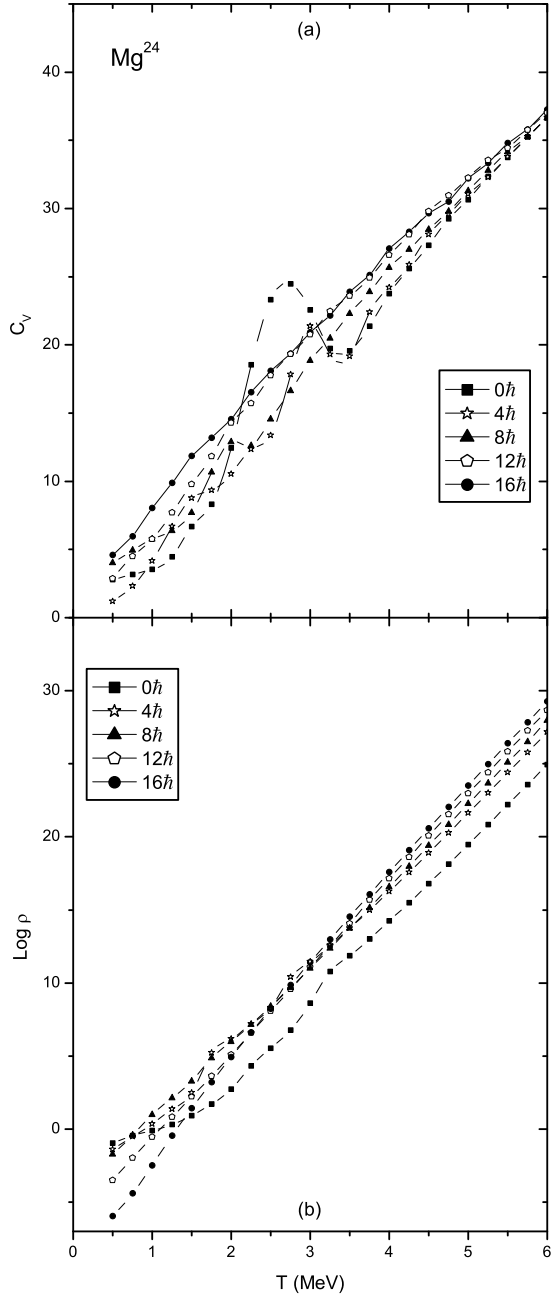


Fig. 8. (a) As in Fig. 5 (a) for ^{24}Mg . (b) As in Fig. 5 (b) for ^{24}Mg .

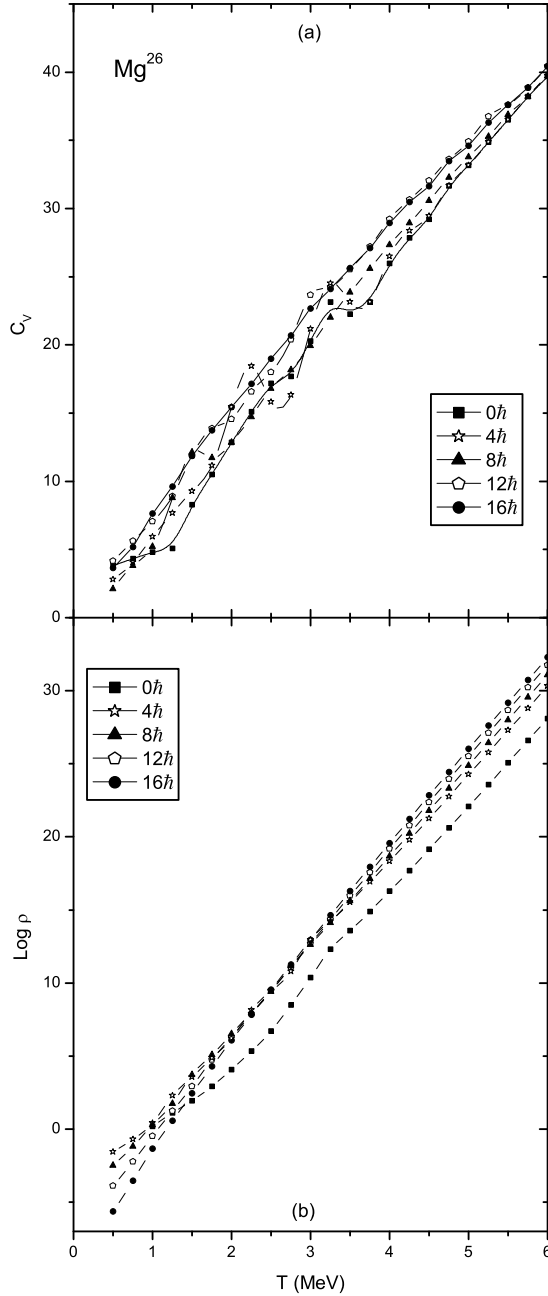


Fig. 9. (a) As in Fig. 5 (a) for ^{26}Mg . (b) As in Fig. 5 (b) for ^{26}Mg .

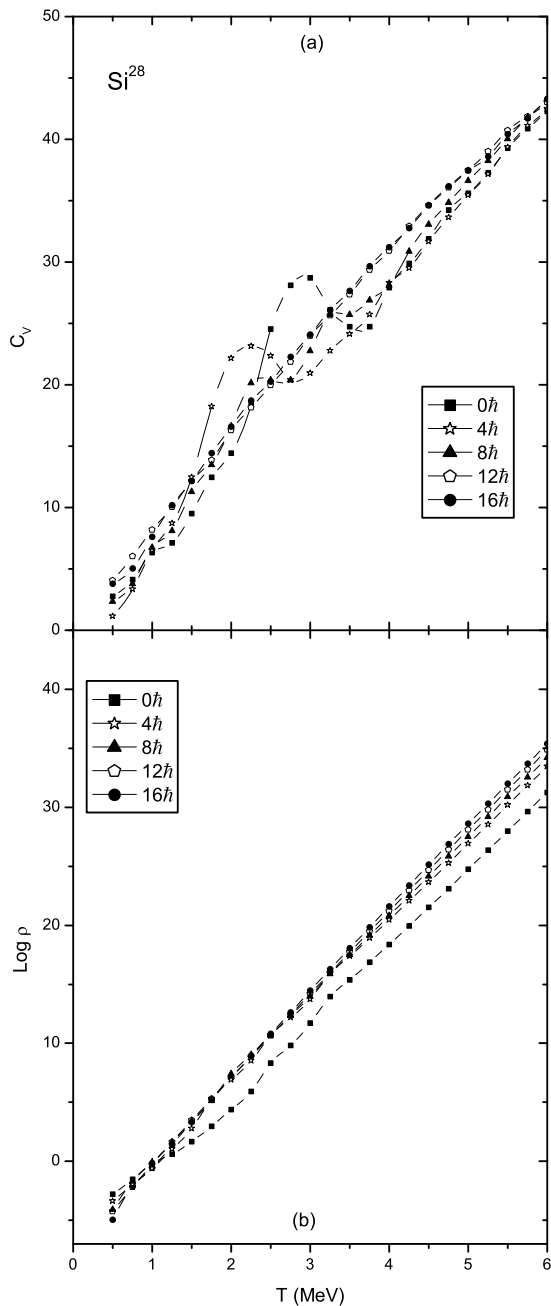


Fig. 10. (a) As in Fig. 5 (a) for ^{28}Si . (b) As in Fig. 5 (b) for ^{28}Si .

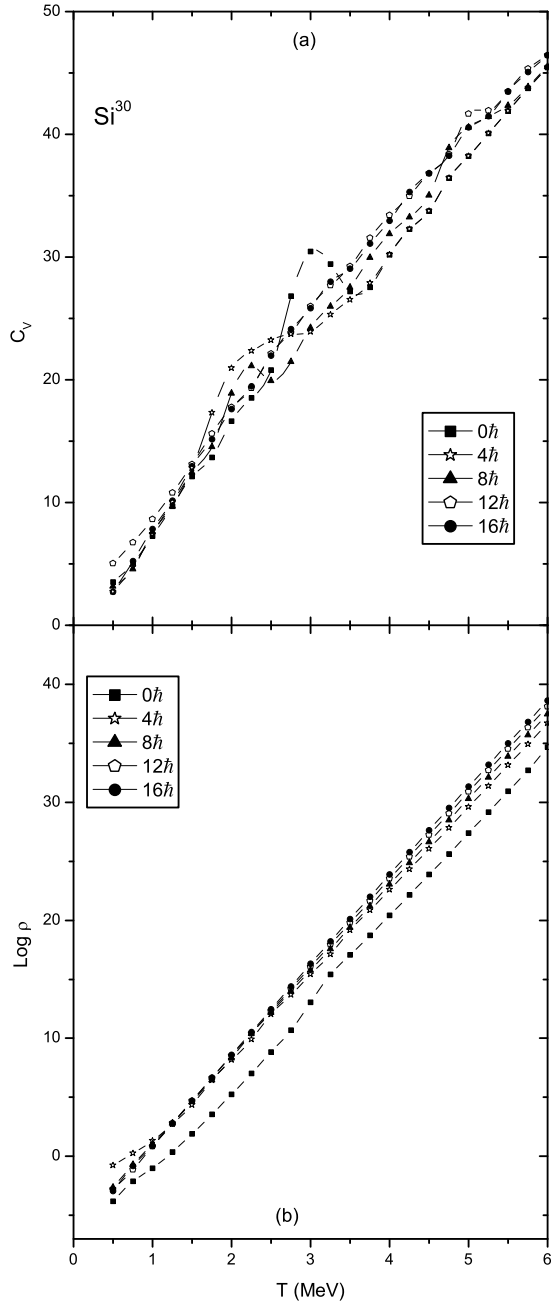


Fig. 11. (a) As in Fig. 5 (a) for ^{30}Si . (b) As in Fig. 5 (b) for ^{30}Si .

Figures 5 (a) to 11 (a) show the dependence of angular momentum and temperature on specific heat and Figs. 5 (b) to 11 (b) show the corresponding level density calculations for all the seven nuclei independently. The effect of angular momentum on specific heat and level density is very well pronounced at low temperatures. This is clearly shown in Fig. 8 for $^{24}_{12}\text{Mg}$ at different angular momentum states. As the angular momentum increases beyond $8\hbar$, the peak occurs at critical temperature between $I = 0\hbar$ and $8\hbar$ vanishes. Similar effects are observed in all the other light nuclei. The specific heat values are different for different angular momentum states of the nuclei at high temperatures.

The incidence of a bump in the specific heat may be due to a nuclear structure effect leading to a phase transition. Comparable structures are seen in specific heat which strengthens the fact that such phase transitions do occur [17]. Additionally, the critical temperature is predicted outstandingly well in finite temperature mean field calculations even in small model spaces [56]. Such transitions are interpreted as thermal excitations from collective to non-collective portions of the nuclear spectrum. As the system heats up, it has a tendency to become less deformed on average and at a specific critical temperature it experiences a deformed to spherical phase transition. Therefore, it is evident that the occurrence of the peak in the specific heat with the high temperature contribution of the ground state rotational band is associated with a deformed to spherical phase transition.

This work is supported by a project (No. 2012/37P/37/BRNS/2017) sanctioned under the Department of Atomic Energy Board of Research in Nuclear Science, India.

REFERENCES

- [1] H.-B. Bai, X.-W. Li, *Chin. Phys.* **C35**, 925 (2011).
- [2] K. Van Houcke, S.M.A. Rombouts, K. Heyde, Y. Alhassid, *Phys. Rev.* **C79**, 024302 (2009).
- [3] F. Iachello, A. Leviatan, D. Petrellis, *Phys. Lett.* **B705**, 379 (2011).
- [4] W. Dilg *et al.*, *Nucl. Phys.* **A217**, 269 (1973).
- [5] J. Johansson, *Phys. Lett.* **A372**, 6301 (2008).
- [6] S. Levit, Y. Alhassid, *Nucl. Phys.* **A413**, 439 (1984).
- [7] J.L. Egido, P. Ring, *J. Phys. G. Nucl. Part. Phys.* **19**, 1 (1993).
- [8] A.L. Goodman, *Nucl. Phys.* **A352**, 30 (1981); J.L. Egido, P. Ring, S. Iwasaki, H.J. Mang, *Phys. Lett.* **B154**, 1 (1985).
- [9] H.G. Miller, R.M. Quick, G. Bozzolo, J.P. Vary, *Phys. Lett.* **B118**, 13 (1986).

- [10] T.R. Rajasekaran, G. Kanthimathi, *Eur. Phys. J.* **A35**, 57 (2008).
- [11] R.K. Pathria, *Statistical Mechanics*, Pergamon, Oxford 1972, pp. 76, 159, 195.
- [12] K. Tanabe, K. Sugawara-Tanabe, *Phys. Lett.* **B97**, 337 (1980); *Nucl. Phys.* **A390**, 385 (1982).
- [13] A.L. Goodman, *Phys. Rev.* **C29**, 1887 (1984).
- [14] R.K. Bhaduri, W. Van Dijk, *Nucl. Phys.* **A485**, 1 (1998).
- [15] B.J. Cole, R.M. Quick, H.G. Miller, *Phys. Rev.* **C40**, 456 (1989).
- [16] H.G. Miller, R.M. Quick, B.J. Cole, *Phys. Rev.* **C39**, 1599 (1989).
- [17] H.G. Miller, B.J. Cole, R.M. Quick, *Phys. Rev. Lett.* **63**, 1922 (1989).
- [18] G.D. Yen, H.G. Miller, *Phys. Lett.* **B192**, 1 (1992).
- [19] J. Dukelsky, A. Poves, J. Retamosa, *Phys. Rev.* **C44**, 2872 (1991).
- [20] O. Civitarese, M. Schevellingner, *Phys. Rev.* **C49**, 1 (1994).
- [21] E. Davis, H.G. Miller, *Phys. Lett.* **B196**, 277 (1987).
- [22] Nguyen Quang Hung, *Proc. Natl. Conf. Theor. Phys.* **36**, 95 (2011).
- [23] R. Rossignoli, A. Plastino, *Phys. Rev.* **C32**, 1040 (1985).
- [24] R. Rossignoli, A. Ansari, P. Ring, *Phys. Rev. Lett.* **70**, 1061 (1993).
- [25] P. Cejnar, *Phys. Rev.* **C65**, 044312 (2002).
- [26] A.V. Afanasjev, J. Konig, P. Ring, *Phys. Rev.* **C62**, 054306 (2000).
- [27] J. Kvasil, R.G. Nazmitdinov, *Phys. Rev.* **C73**, 014312 (2006).
- [28] M. Hasegawa, K. Kaneko, T. Mizusaki, Y. Sun, *Phys. Lett.* **B656**, 51 (2007).
- [29] H. Nakada, Y. Alhassid, *Phys. Rev. Lett.* **79**, 2939 (1997).
- [30] J. Bardeen, L.N. Cooper, J.R. Schrieffer, *Phys. Rev.* **108**, 1175 (1957).
- [31] J. des Cloizeaux, *Many-Body Physics*, ed. C. de Will, R. Balian, Gorden and Breach, New York 1968.
- [32] A.L. Goodman, *Phys. Lett.* **B131**, 5 (1983).
- [33] V. Martin, J.L. Egido, L.M. Robledo, *Phys. Rev.* **C68**, 034327 (2003).
- [34] K. Esashika, H. Nakada, K. Tanabe, *Phys. Rev.* **C72**, 044303 (2005).
- [35] C. Ozen, Y. Alhassid, H. Nakada, *Phys. Rev. Lett.* **110**, 042502 (2013).
- [36] R. Rossignoli, N. Canosa, P. Ring, *Phys. Rev. Lett.* **80**, 1853 (1998).
- [37] S. Liu, Y. Alhassid, *Phys. Rev. Lett.* **87**, 022501 (2001).
- [38] G. Kanthimathi, N. Boomadevi, T.R. Rajasekaran, *Commun. Theor. Phys.* **56**, 718 (2011).
- [39] M. Rajasekaran, T.R. Rajasekaran, N. Arunachalam, V. Devanathan, *Phys. Rev. Lett.* **61**, 2077 (1988); M. Rajasekaran, N. Arunachalam, T.R. Rajasekaran, V. Devanathan, *Phys. Rev.* **C38**, 1926 (1988).

- [40] M. Rajasekaran, T.R. Rajasekaran, N. Arunachalam, *Phys. Rev.* **C37**, 307 (1988); M. Rajasekaran, N. Arunachalam, T.R. Rajasekaran, V. Devanathan, *Pramana J. Phys.* **32**, 515 (1989); T.R. Rajasekaran, S. Selvaraj, S. Santhosh Kumar, *Pramana J. Phys.* **60**, 75 (2003).
- [41] J.R. Heuizenga, L.G. Moretto, *Annu. Rev. Nucl. Sci.* **22**, 427 (1972); L.G. Moretto, *Nucl. Phys.* **A182**, 641 (1972); **A185**, 145 (1972); **A216**, 1 (1973).
- [42] K.-H. Schmidt, B. Jurado, *Phys. Rev.* **C86**, 044322 (2012).
- [43] M. Aggarwal, S. Kailas, *Phys. Rev.* **C81**, 047302 (2010).
- [44] A.N. Behkami, Z. Kargar, N. Nasrabadi, *Phys. Rev.* **C66**, 064307 (2002).
- [45] D. Bucurescu, T.V. Egidy, *J. Phys. G. Nucl. Part. Phys.* **31**, 1675 (2005).
- [46] V.M. Strutinsky, *Nucl. Phys.* **A95**, 420 (1967).
- [47] P.J. Brancazio, A.G.W. Cameron, *Can. J. Phys.* **47**, 1029 (1969).
- [48] Y. Alhassid, *AIP Conf. Proc.* **769**, 1283 (2005) [arXiv:nucl-th/0604069].
- [49] D. Mocolj *et al.*, *Phys. Rev.* **C75**, 045805 (2007).
- [50] P. Moller, J.R. Nix, W.D. Myers, W.D. Swiatecki, *At. Data Nucl. Data Tables* **59**, 185 (1995).
- [51] S.G. Nilsson *et al.*, *Nucl. Phys.* **A131**, 1 (1969); G. Shunmugam, P.R. Subramaniam, M. Rajasekaran, V. Devanathan, in *Nuclear Interactions*, Vol. 92 of Lecture Notes in Physics, ed. B.A. Rapson, Springer, Berlin 1979, p. 433.
- [52] P.A. Seegar, Proceedings of the International Conference on the Properties of Nuclei Far From the Region of Beta Stability, Switzerland, 1970.
- [53] J.M. Eisenberg, W. Greiner, *Microscopic Theory of the Nucleus*, North Holland, Amsterdam 1976, p. 399; T. Bengtsson, *Nucl. Phys.* **A496**, 56 (1989).
- [54] K. Snover, *Annu. Rev. Part. Nucl. Sci.* **36**, 545 (1986).
- [55] S. Henss *et al.*, *Phys. Rev. Lett.* **60**, 11 (1988).
- [56] R.M. Quick, N.J. Davidson, B.J. Cole, H.G. Miller, *Phys. Lett.* **B254**, 303 (1991).